ELSEVIER

Journal of Power Sources 104 (2002) 108–114

JOURNAL OF POWER SOURCES

www.elsevier.com/locate/jpowsour

Electrochemical behavior of plasma-fluorinated graphite for lithium ion batteries

Tsuyoshi Nakajima[a,*], Vinay Gupta[a], Yoshimi Ohzawa[a], Meiten Koh[b], Ram Niwas Singh[b], Alain Tressaud[c], Etienne Durand[c]

[a]*Department of Applied Chemistry, Aichi Institute of Technology, Yakusa-cho, Toyota-shi 470-0392, Japan*
[b]*Department of Polymer Chemistry, Kyoto University, Sakyo-ku, Kyoto 606-8501, Japan*
[c]*ICMCB-CNRS, Université Bordeaux I, 87Avenue Dr. A. Schweitzer; 33608 Pessac Cedex, France*

Received 26 March 2001; received in revised form 6 August 2001; accepted 9 August 2001

Abstract

Electrochemical properties of plasma-fluorinated graphite samples have been investigated in 1 mol dm^{-3} $LiClO_4$ ethylene carbonate (EC)/diethyl carbonate (DEC) solution at 25 °C. Fluorine contents in plasma-fluorinated graphite samples were in the range of 0–0.3 at.% by elemental analysis and surface fluorine concentrations obtained by X-ray photoelectron spectroscopy (XPS) were in the range of 3–12 at.%. Raman spectroscopy revealed that surface disordering of graphite was induced by plasma fluorination. Plasma treatment increased the surface areas of graphite samples by 26–55% and the pore volumes for the mesopores with diameters of 1.5–2 and 2–3 nm. Plasma-fluorinated graphites showed capacities higher than those of original graphites and even higher than the theoretical capacity of graphite, 372 mAh g^{-1}, without any change of the profile of charge–discharge potential curves. The increments in the capacities were approximately 5, 10 and 15% for graphites with average particle diameters, 7, 25 and 40 μm, respectively. Furthermore, the coulombic efficiencies in first cycle were nearly the same as those for original graphites or higher by several percents.

Keywords: Plasma fluorination; Surface modification; Graphite electrode; Lithium ion battery

1. Introduction

Surface modification of carbon materials as anodes in lithium ion secondary batteries is of decisive importance because during the intercalation/de-intercalation process lithium ions interact with the chemical species existing at the edge plane of carbon materials. The chemical species at the surface such as hydroxyl and carboxyl groups react with lithium at the beginning in first charge process of a battery; forming a solid electrolyte interphase by decomposing organic solvents [1]. Crystallinity; surface structure, surface area and also nature of surface species are important factors influencing the electrochemical decomposition of organic solvents in the charging process [2]. Hydrogen atoms existing at the edge plane of carbon material cause large hysteresis in potential curves [3]. Several surface modifications were applied to carbon materials in order to increase the electrochemical reaction rate and capacity [1,4–9], i.e. surface oxidation [1,4,5], surface fluorination [6,7], high temperature treatment under vacuum [8] and metal coating [9]. Light oxidation of graphite and carbon gives rise to an increase in the capacities due to the formation of nanopores through which solvating organic molecules are not allowed to pass. On the other hand, strong oxidation causes degradation of carbon materials and yields a large amount of surface oxygen species leading to an increase in the irreversible capacity [1,5]. Surface oxidation of mesocarbon microbeads (MCMBs) is effective for removing the surface skin, thus, increasing the reaction rate [4]. Heating of carbon materials to ~1000 °C under vacuum also increases both electrochemical reaction rates and capacities by reducing the number of surface oxygen species [8]. Metal coating is another method to activate the surface of carbon materials and increase the reaction rate [9]. Surface fluorination of graphite by elemental fluorine has been attempted by some of us and capacities of surface-fluorinated graphites have been found to exceed the theoretical value of graphite, 372 mAh g^{-1} [7]. The objectives of surface fluorination are to enlarge the electrode surface area and to modify the surface pore structure of graphite. When graphite surface

* Corresponding author. Tel.: +81-565-48-8121/ext. 2201; fax: +81-565-48-0076.
E-mail address: nakajima@ac.aitech.ac.jp (T. Nakajima).

0378-7753/02/$ – see front matter
PII: S0378-7753(01)00895-3

is fluorinated by elemental fluorine, fluorination should be performed with fluorine gas at a low pressure for several minutes between 150 and 500 °C. This temperature range is necessary to avoid the intercalation of fluorine into graphite which takes place at a temperature below ca. 100 °C and the formation of thick fluorinated graphene layers which occurs at higher temperatures because both kinds of reactions lead to an increase in irreversible capacity [7]. Plasma fluorination using a fluoride gas such as CF_4 would be another effective method of surface modification. In this paper, we report the electrochemical properties of plasma-fluorinated graphite samples in organic solvents and discuss on the relation between the electrochemical characteristics and surface structures of graphite.

2. Experimental

2.1. Radiofrequency plasma fluorination of graphite

Graphite samples with average particle diameters 7, 25 and 40 μm were treated in a fluorinated plasma obtained from CF_4 gas excited by a radiofrequency (rf) source at 13.56 MHz. The reactor was formed of two aluminum barrel electrodes which were coated with alumina. The inner electrode on which the sample was placed was connected to the rf source and the outer one was grounded. A primary vacuum was obtained by a 40 $m^3\ h^{-1}$ pump equipped with a liquid nitrogen condenser in order to trap the residual gases. The gas was introduced in the upper part of the reactor and then dissociated by electron impacts occurring between the two electrodes. Neutral species and radicals diffused from on a PTFE disk. The chamber was thermostatically controlled and a temperature lower than 100 °C was maintained during the process.

Several experimental parameters could be adjusted during the plasma-enhanced fluorination (PEF) experiments, namely, the inlet gas flow, 8 $cm^3\ min^{-1}$; the total pressure, 3.4 Pa; the rf power, 80 W; and the reaction duration, 30–180 min [10,11].

2.2. Analyses of plasma-fluorinated graphite samples

Structure change of plasma-fluorinated graphite samples were examined by X-ray diffractometry (Shimadzu, XD-610 with Cu Kα radiation). The fluorine contents of plasma-fluorinated graphite samples were analyzed by elemental analysis of carbon and fluorine at Elemental Analysis Center of Faculty of Pharmaceutical Science of Kyoto University. The detection limit of fluorine by elemental analysis is within 0.3 wt.%. The amount of oxygen was calculated by subtracting the analytical values for carbon and fluorine from 100 wt.%. Surface compositions were determined from the peak areas of C 1s, F 1s and O 1s spectra obtained by X-ray photoelectron spectroscopy (XPS, Ulvac Phi Model 5500 with Mg Kα radiation). The nature of C–F bonding was also checked by XPS. The binding energies of photoelectron peaks were determined relative to that of C 1s electron of graphite, 284.3 eV without charging correction. Surface disordering of graphite by plasma fluorination was investigated by Raman spectroscopy (Jobin-Yvon, T-64000 with Ar ion laser of 514.5 nm). The peak intensity ratios in Raman spectra were calculated as R values to evaluate the degree of surface disordering. Surface areas and pore volume distribution of graphite samples were measured by BET method using nitrogen gas (Micromeritics, Gemini 2375). Plasma-fluorinated graphite samples for the surface structure analysis were prepared by 60 min fluorination.

2.3. Electrochemical measurement of plasma-fluorinated graphite

The galvanostatic charge–discharge cycling for plasma-fluorinated graphite electrode was made at 25 °C by using three electrodes glass cell in a glove box filled with argon. The method of graphite electrode preparation was described in a previous paper [7]. The counter and reference electrodes were metallic lithium, and electrolyte solution was 1 mol dm^{-3} $LiClO_4$ ethylene carbonate (EC)/diethyl carbonate (DEC) (1:1, v/v). The charge–discharge cycling was performed at a current density of 60 mA g^{-1} between 0 and 3 V versus Li/Li^+.

3. Results and discussion

3.1. Surface compositions and structure change of plasma-fluorinated graphite samples

Fluorine contents in plasma-fluorinated graphite samples were 0.3 at.% or within detection limit (0.3 wt.% or 0.2 at.%) under the fluorination conditions adopted as given in Table 1. The surface fluorine concentrations obtained by

Table 1
Composition of plasma-fluorinated graphite samples, obtained by elemental analysis and calculated from peak areas of X-ray photoelectron spectra

Sample	Fluorination time (min)	Elemental analysis (at.%)			XPS (at.%)		
		C	F	O	C	F	O
1[a]	30	–	–	–	90.8	6.9	2.3
2[a]	60	99.9	0.0	(0.1)	90.3	7.5	2.2
3[a]	100	99.7	0.0	(0.3)	90.6	7.8	1.6
4[a]	140	99.7	0.0	(0.3)	92.0	6.7	1.3
5[a]	180	99.8	0.0	(0.2)	91.3	7.7	1.0
6[b]	60	99.6	0.3	(0.1)	90.1	7.1	2.8
7[b]	60	99.5	0.3	(0.2)	86.3	11.5	2.2
8[c]	60	99.6	0.3	(0.1)	94.8	3.3	1.9

[a] Natural graphite with average diameter of 7 μm (NG-7).
[b] Natural graphite with average diameter of 25 μm (NG-25).
[c] Natural graphite with average diameter of 40 μm (NG-40). Sample 6 was fluorinated at room temperature. All other samples were fluorinated at about 90 °C. Values inside parentheses are calculated by subtracting the analytical values for carbon and fluorine from 100 wt.%.

XPS were, however; much higher (7–9 at.%) in most of the samples though small amounts of surface oxygen (1–3 at.%) were also detected. It can be noted that both the fluorine contents obtained by elemental analysis and the surface fluorine concentrations obtained by XPS were lower in these samples than those of graphites fluorinated by elemental fluorine on the average [7]. Furthermore, the plasma-fluorinated graphite samples exhibited more constant surface concentrations than those fluorinated by elemental fluorine. These data suggest that rf plasma fluorination yields thin fluorinated layers at the surface of graphite. The surface oxygen concentrations of plasma-fluorinated samples were also lower than the values for graphites fluorinated by elemental fluorine, and moreover, these values decrease with increasing fluorination duration. These results coincide with those obtained by Raman spectroscopy as discussed later.

X-ray diffraction measurements of plasma-fluorinated graphite samples have shown that the profiles of X-ray diffractograms are nearly the same as those of original graphites.

Typical photoelectron spectra of C 1s, F 1s and O 1s levels are shown in Fig. 1. C 1s spectra have their main peaks at 284.3 eV with low intensity peaks at 285.3, 288.1 ± 0.3 and 291.1 ± 0.1 eV. Among them, the two last peaks are correlated with C–F bonding [7,12–16]. The peak at 288.1 ± 0.3 eV indicates tertiary carbon atoms bonded to fluorine, C–F, and a small amount of carboxyl groups. The peak at 291.1 ± 0.1 eV indicates the presence of a trace amount of carbon covalently bonded to fluorine and a plasmon satellite. The other C 1s peak at 285.3 eV is due to carbon atom neighboring to that bonded to fluorine and a small amount of carbon atom bonded to hydroxyl or carbonyl group. F 1s peak corresponding to the C 1s peak shifted to 288.1 ± 0.3 eV is observed at 687.6 ± 0.2 eV which is an intermediate value between those for semi-ionic and covalent C–F bonds [7,12–16]. Weak O 1s peaks are also observed at 531.5 ± 0.5 and 533.6 ± 0.3 eV indicating carbonyl and hydroxyl groups, respectively. All these peak positions are nearly the same as those observed for graphites fluorinated by elemental fluorine [7], that is, C–F bonding is in an intermediate state between semi-ionic and covalent bonds [7,12–16].

Raman spectroscopy distinguishes ordered and disordered structures for the surface region of carbon materials. A band observed at 1580 cm^{-1} arises from an E_{2g2} vibration mode in the graphitic region of carbon materials (G-band) while another band at 1360 cm^{-1} is due to an A_{1g} mode in the disordered region of carbon materials or edge plane of powdery carbon (D-band) [17,18]. The ratio of intensity of D-band to that of G-band ($R = I_D/I_G$) well indicates the degree of disordering of surface area of carbon materials. Fig. 2 shows the Raman spectrum of original graphite (average particle diameter, 7 μm) and a typical one of plasma-fluorinated graphite. The profile and peak positions of Raman bands are not modified by plasma fluorination except for a slight increase in the D-band intensity as in the

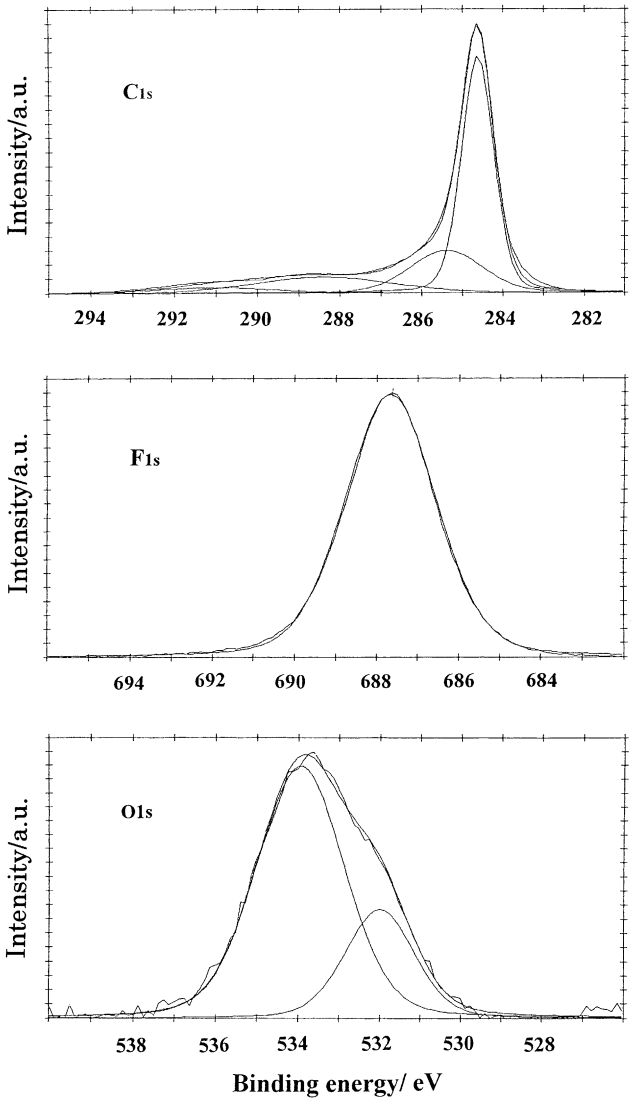

Fig. 1. X-ray photoelectron spectra of 60 min-fluorinated graphite (sample 2 in Table 1).

case of fluorination by elemental fluorine [7]. The increase in the R values is slightly smaller in plasma fluorination as given in Table 2 (R values are in the range of 0.13–0.20) while they were observed in the range of 0.15–0.40 in case of the fluorination by elemental fluorine [7]. Among three graphite samples having different particle diameters, R values of original graphites and plasma-fluorinated ones are only slightly influenced by the increase in the average particle diameter. Another interesting point for plasma fluorination is that R value decreases from 0.20 to 0.13 with increasing duration of plasma fluorination. This means that the surface disordering induced by plasma fluorination is somewhat reduced by further plasma treatment, which would partially eliminate the disordered surface of graphite.

The increase in R values of Raman spectra by plasma fluorination suggests the enlargement of surface area of

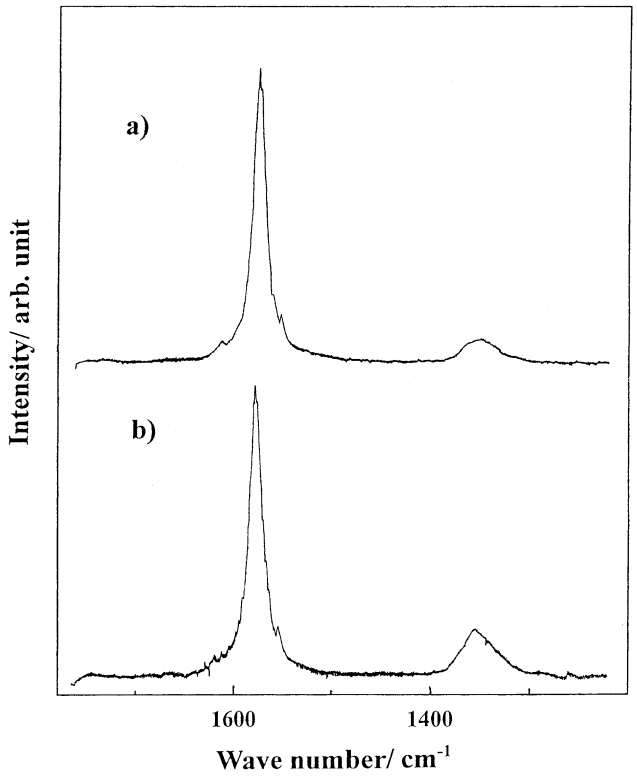

Fig. 2. Raman spectra of original graphite (average particle diameter, 7 μm) (a) and 60 min-fluorinated graphite (sample 2 in Table 1) (b).

graphite electrode and formation of surface pores. In fact, the surface areas of graphite samples increased by plasma treatment as given in Table 3. The increase in the surface areas was 55, 27 and 26% for 7, 25 and 40 μm graphite samples. Pore volume distribution was also significantly changed as given in Table 4. Original graphite samples have mesopores with diameters of 1.5–2 to 8–10 nm. Their distribution is rather uniform, though the mesopores with

Table 2
R (I_D/I_G) values from Raman spectra of plasma-fluorinated graphite samples

Sample	R value
NG-7	0.083
2[a]	0.20
3[a]	0.14
4[a]	0.13
5[a]	0.13
NG-25	0.082
6[b]	0.14
7[b]	0.15
NG-40	0.080
8[c]	0.14

[a] Natural graphite with average diameter of 7 μm (NG-7).
[b] Natural graphite with average diameter of 25 μm (NG-25).
[c] Natural graphite with average diameter of 40 μm (NG-40). Sample 6 was fluorinated at room temperature. All other samples were fluorinated at about 90 °C.

Table 3
Surface areas of 60 min-fluorinated graphite samples

Graphite sample	Surface area ($m^2\ g^{-1}$)		
	NG-7	NG-25	NG-40
Original	4.79	3.71	2.94
60 min-fluorinated	7.42	4.71	3.69

diameters of 2–3 and 3–4 nm are relatively larger. However, the plasma fluorination increased the volumes of mesopores with diameters of 1.5–2 and 2–3 nm to about four and two times, respectively. On the contrary, the mesopores with diameters of 3–4 nm were drastically decreased and other mesopores with diameters larger than 3–4 nm completely disappeared. The change of pore volume distribution may be attributed to the destruction of C–C bonds of graphite by plasma fluorination. The increase in the surface areas of graphite samples would increase the reaction rate at electrode surface, and the mesopores with diameters of 1.5–2 and 2–3 nm may accommodate some amount of excess lithium as shown later.

3.2. Electrochemical properties of plasma-fluorinated graphite samples

The plasma-fluorinated graphite samples have almost the same potential profile as that of original graphite (≈7 μm) as shown in Fig. 3. A small potential plateau is observed at 0.7 V indicating the electrochemical decomposition of the solvents containing EC only in the first reduction process [2]. No such a plateau is observed from second cycle due to a film formation onto the graphite surface. The electrode potential is low and flat during lithium ion intercalation and de-intercalation reactions. The charge capacities (discharge capacity in a practical lithium ion battery) are slightly increased after first cycle, reaching constant values after several cycles for all the plasma-fluorinated samples. This would be caused by removal of surface fluorine atoms due to the reaction with lithium. The charge capacities of

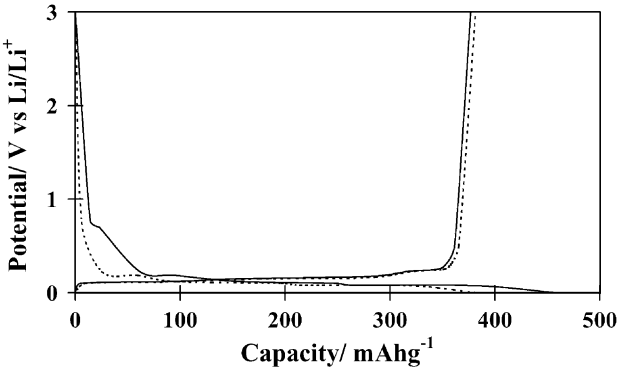

Fig. 3. Charge–discharge curves of 60 min-fluorinated graphite (sample 2 in Table 1): first cycle (—); tenth cycle (· · ·).

Table 4
Pore volume distribution of 60 min-fluorinated graphite samples

Pore diameter (nm)	Pore volume ($\times 10^{-9}$ m^3 g^{-1})					
	NG-7		NG-25		NG-40	
	Original	Fluorinated	Original	Fluorinated	Original	Fluorinated
1.5–2	0.23	1.08	0.20	0.74	0.14	0.51
2–3	1.22	2.60	0.81	1.62	0.75	1.40
3–4	1.05	0.04	0.68	0.02	0.58	0.02
4–5	0.76	–	0.50	–	0.43	–
5–6	0.54	–	0.39	–	0.36	–
6–8	1.08	–	0.77	–	0.40	–
8–10	0.30	–	0.23	–	–	–

plasma-fluorinated graphite samples (≈7 μm) are highly dependent on the duration of plasma fluorination (Fig. 4). The 30 min-fluorinated sample shows capacities of about 370 mAh g^{-1}, higher than that of original graphite, 364 mAh g^{-1}. The 60 min-fluorinated graphite gave 382 mAh g^{-1} which is the largest among NG-7 μm graphite samples. This value is larger than not only that of original graphite, but also the theoretical capacity of graphite, 372 mAh g^{-1}, which is the capacity corresponding to the stage 1 lithium-intercalated graphite, LiC_6. When the duration of fluorination is further extended to 100–180 min, the charge capacities decrease to values comparable to that of original graphite. The optimum duration of plasma fluorination, is thus, 60 min under the conditions examined. The obtained charge capacities are closely related to *R* values of Raman spectra, given in Table 2. The plasma-fluorinated graphites having the larger *R* values have shown the higher capacities. The small *R* values arise from the elimination of surface disordered layers by the excess plasma fluorination, which suggests a decrease in the surface areas and volumes of mesopores of graphite samples. These surface structure changes may reduce the reaction rates and excess lithium preserved in surface mesopores.

With increase in the particle size, the capacities of original graphites decrease, i.e. the capacity of 25 μm graphite was 355 mAh g^{-1} and that of 40 μm graphite was 333 mAh g^{-1}, while that of 7 μm graphite was 364 mAh g^{-1}. The surface area of graphite decreases with increase in the particle size as given in Table 3. This structural factor reduces the intercalation and de-intercalation rates of lithium ion into and from graphite with increasing particle size. The 60 min plasma-fluorinated graphite samples have in any case much higher charge capacities than those of untreated graphites and the theoretical value of graphite, 372 mAh g^{-1} as shown in Figs. 4–6. The effect of surface fluorination becomes more distinct as the particle size increases. Charge capacities increased from 364, 355 and 333 mAh g^{-1} to 382, 388 and 381 mAh g^{-1} for 7, 25 and 40 μm graphites, respectively. The increase of charge capacities by plasma fluorination, was thus 5, 10 and 15% for 7, 25 and 40 μm graphite

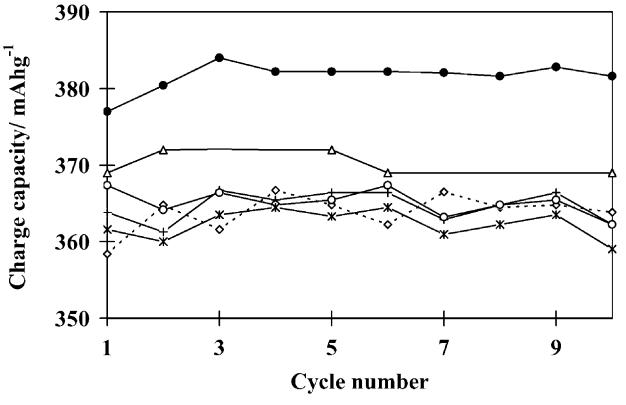

Fig. 4. Charge capacities of plasma-fluorinated graphite samples as a function of cycle number: original graphite (average particle diameter, 7 μm) (◇); 30 min-fluorinated graphite (sample 1 in Table 1) (△); 60 min-fluorinated graphite (sample 2 in Table 1) (●); 100 min-fluorinated graphite (sample 3 in Table 1) (+); 140 min-fluorinated graphite (sample 4 in Table 1) (○); 180 min-fluorinated graphite (sample 5 in Table 1) (✱).

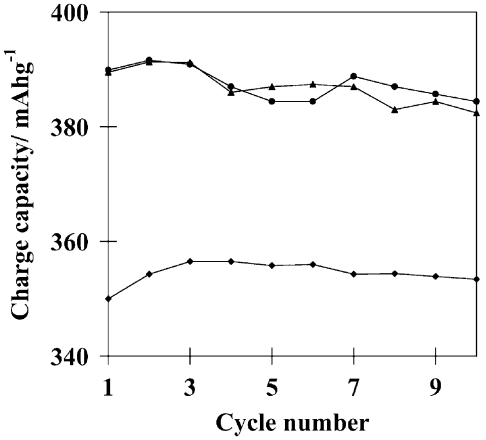

Fig. 5. Charge capacities of plasma-fluorinated graphite samples as a function of cycle number: original graphite (average particle diameter, 25 μm) (◆); 60 min-fluorinated graphite at room temperature (sample 6 in Table 1) (●); 60 min-fluorinated graphite at 90 °C (sample 7 in Table 1) (▲).

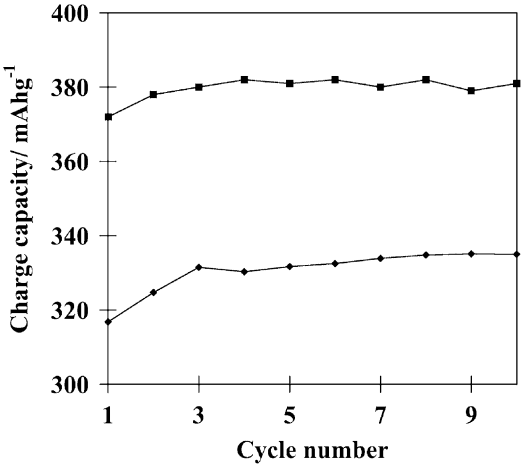

Fig. 6. Charge capacities of plasma-fluorinated graphite as a function of cycle number: original graphite (average particle diameter, 40 μm) (◆); 60 min-fluorinated graphite (sample 8 in Table 1) (■).

samples, respectively. As shown in Table 3, the increase in the surface areas of graphite samples by plasma fluorination is 26–55%. The enlargement of surface area would accelerate the reaction kinetics so that the full space of graphene layers may be used for accommodation of lithium. The observed capacities were 381–388 mAh g^{-1} which are nearly the same values irrespective of the particle sizes of graphite samples. This suggests that not only the full space of plasma-fluorinated graphite is used as an electrode, but also some excess lithium is stored in the surface mesopores created by plasma fluorination.

It has been also found that first coulombic efficiencies are the same as those of original graphites, or slightly higher as given in Table 5. The higher coulombic efficiencies in first cycle were observed in some plasma-fluorinated graphite samples with average particle diameter of 7 μm. Total fluorine contents were in the range of 0–0.3 at.%, being lower in plasma-fluorinated samples than those fluorinated by elemental fluorine [7], and surface fluorine concentrations were also somewhat lower, i.e. 7–9 at.%, in most of the samples. The plasma-fluorinated samples contain surface oxygen of 1–3 at.% as mentioned in the previous section. Since the similar amounts of oxygen are detected for original graphite samples, the influence of surface oxygen on the coulombic efficiency would be negligible.

From these electrochemical data, it is clear that surface fluorination effectively modifies the surface structures, i.e. not only enhances the reaction rates, but also makes possible the preservation of larger amount of lithium than that in the first stage, LiC_6. Lithium ion intercalation and de-intercalation would mainly occur through edge plane of graphite. It is also possible for lithium ion to pass through the cracks which can be formed on the basal plane by plasma fluorination. Oxygen species such as hydroxyl, carbonyl and carboxyl groups would be mainly bonded to carbon atoms at the edge plane of graphite and in some parts, the external surface may be capped by C–C bonds in the similar manner than those found for carbon nanotubes [19]. Plasma fluorination effectively modifies such surface structure of graphite: some amount of oxygen species may be replaced by fluorine and closed external surface may be opened by the break of C–C bonds, followed by subsequent formation of C–F bonds. At the same time, the surface areas of graphite samples are enlarged and the mesopores with diameters of 1.5–2 and 2–3 nm are significantly increased by plasma fluorination as already shown. The enlargement of electrode surface would improve the reaction kinetics and the surface mesopores can store some amount of excess lithium. The improvement of reaction kinetics is evident for graphite samples having the larger diameters, 25 and 40 μm as shown in Figs. 5 and 6.

Table 5
Coulombic efficiencies (%) of plasma-fluorinated graphite samples

Sample	Cycle number									
	1	2	3	4	5	6	7	8	9	10
NG-7	80.8	92.8	96.7	96.4	97.8	98.3	98.4	98.6	99.3	97.2
1[a]	83.8	96.2	–	–	97.7	–	99.2	–	–	99.2
2[a]	80.2	96.0	97.6	98.0	98.5	98.5	98.9	98.8	99.0	99.7
3[a]	84.3	95.2	97.5	98.5	99.3	99.3	99.2	99.8	99.7	99.4
4[a]	85.7	95.6	97.7	98.4	99.7	99.7	99.6	99.1	99.7	99.7
5[a]	84.8	96.6	97.0	99.0	99.5	99.1	99.3	99.7	99.7	99.3
NG-25	85.6	95.0	96.6	97.4	97.4	97.6	98.1	98.1	98.2	98.4
6[b]	85.4	95.6	97.4	97.5	97.8	97.9	98.5	98.7	98.1	98.0
7[b]	85.8	95.7	97.1	97.2	97.7	98.0	98.1	98.7	98.6	98.7
NG-40	85.1	93.4	95.4	96.2	96.7	97.5	97.8	98.0	98.3	98.8
8[c]	84.0	94.0	96.0	96.7	98.0	98.2	97.5	98.5	98.5	98.2

[a] Natural graphite with average diameter of 7 μm (NG-7).
[b] Natural graphite with average diameter of 25 μm (NG-25).
[c] Natural graphite with average diameter of 40 μm (NG-40). Sample 6 was fluorinated at room temperature. All other samples were fluorinated at about 90 °C.

4. Conclusion

It has been shown in the present study that plasma fluorination is an effective method of surface modification of graphite electrode for lithium ion secondary battery. The reaction kinetics can be significantly improved in particular for graphite samples with diameters of approximately 25 and 40 μm, and the capacities which are approximately 5, 10 and 15% higher than those of original graphites with diameters of approximately 7, 25 and 40 μm, respectively can be obtained. These improvements in the electrochemical properties are attributed to the enlargement of surface areas of graphite samples and the increase in the mesopores with diameters of 1.5–2 and 2–3 nm which may accommodate excess lithium. The fluorine contents in the plasma-fluorinated graphites were low, i.e. within detection limit or only 0.3 at.%, and surface fluorine concentrations obtained from XPS data are almost constant in most of the samples, i.e. 7–9 at.%. The low fluorine contents would be responsible for the high first coulombic efficiencies of plasma-fluorinated graphite samples.

Acknowledgements

The present study is financially supported by grant-in-aid for Research for the Future Program (nanocarbon) of Japan Society for the Promotion of Science and Japan Storage Battery Company, Ltd., which are gratefully acknowledged.

References

[1] E. Peled, C. Menachem, D. Bar-Tow, A. Melman, J. Electrochem. Soc. 143 (1996) L4.
[2] R. Fong, U. von Sacken, J.R. Dahn, J. Electrochem. Soc. 137 (1990) 2009.
[3] T. Zheng, W.R. Mckinnon, J.R. Dahn, Electrochem. Soc. 143 (1996) 2137.
[4] M. Hara, A. Satoh, N. Tamaki, T. Ohsaki, Tanso 165 (1994) 261.
[5] J.S. Xue, J.R. Dahn, J. Electrochem. Soc. 142 (1995) 3668.
[6] T. Nakajima, K. Yanagida, Tanso 174 (1996) 195.
[7] T. Nakajima, M. Koh, R.N. Singh, M. Shimada, Electrochim. Acta 44 (1999) 2879.
[8] T. Takamura, M. Kikuchi, Battery Technol. 7 (1995) 29.
[9] R. Takagi, T. Okubo, K. Sekine, T. Takamura, Denki Kagaku 65 (1997) 333.
[10] F. Moguet, Ph.D. Thesis, University of Bordeaux I, 1996.
[11] T. Shirasaki, E. Moguet, L. Lozano, A. Tressaud, G. Nanse, E. Papirer, Carbon 37 (1999) 1891.
[12] I. Palchan, M. Crespin, H. Estrade-Szwarckopf, B. Rousseau, Chem. Phys. Lett. 157 (1989) 321.
[13] A. Tressaud, C. Guimon, V. Gupta, F. Moguet, Mater. Sci. Eng. B 30 (1995) 61.
[14] Y. Matsuo, T. Nakajima, Z. Anorg. Allg. Chem. 621 (1995) 1943.
[15] T. Nakajima, N. Watanabe, Graphite Fluorides and Carbon–Fluorine Compounds, CRC Press, Boca Raton, FL, 1991.
[16] T. Nakajima (Ed.), Fluorine–Carbon and Fluoride–Carbon Materials, Marcel Dekker, New York, NY, 1995.
[17] F. Tunistra, J.L. Koenig, J. Chem. Phys. 53 (1970) 1126.
[18] D.S. Night, W.B. White, J. Mater. Res. 4 (1989) 385.
[19] K. Moriguchi, S. Munetoh, M. Abe, M. Yonemura, K. Kamei, A. Shintani, Y. Maehara, A. Omaru, M. Nagamine, J. Appl. Phys. 88 (2000) 6369.